

The Arabidopsis ACT7 Actin Gene Is Expressed in Rapidly Developing Tissues and Responds to Several External Stimuli¹

John M. McDowell, Yong-qiang An, Shurong Huang, Elizabeth C. McKinney, and Richard B. Meagher*

Department of Biology, University of North Carolina, Chapel Hill, North Carolina 27599 (J.M.M.); Department of Genetics, University of Georgia, Athens, Georgia 30602–7223 (Y.-q.A., E.C.M., R.B.M.); and Lawrence Berkeley Laboratory, University of California, Berkeley, California 94720 (S.H.)

ACT7 encodes one of the six distinct and ancient subclasses of actin protein in the complex Arabidopsis actin gene family. We determined the sequence and structure of the Arabidopsis thaliana ACT7 actin gene and investigated its tissue-specific expression and regulation. The ACT7 mRNA levels varied by 128-fold among several different tissues and organs. The highest levels of ACT7 mRNA were found in rapidly expanding vegetative organs, the lowest in pollen. A translational fusion with the 5' end of ACT7 (1.9 kb) joined to the β -glucuronidase reporter gene was strongly and preferentially expressed in all young, developing vegetative tissues of transgenic Arabidopsis plants. ACT7 was the only Arabidopsis actin gene strongly expressed in the hypocotyl and seed coat. Although no β -glucuronidase expression was seen in developing ovules or immature seeds, strong expression was seen in dry seeds and immediately after imbibition in the entire seedling. ACT7 was the only Arabidopsis actin gene to respond strongly to auxin, other hormone treatments, light regime, and wounding, and may be the primary actin gene responding to external stimuli. The ACT7 promoter sequence contains a remarkable number of motifs with sequence similarity to putative phytohormone response elements.

Cellular morphogenesis in plants is constrained by rigid cell walls that limit expansion, restrict shape, and prevent migration. Thus, morphogenesis is in part a function of asymmetric cell division and expansion. A number of studies have suggested that these processes are controlled by a dynamic cytoskeleton that consists of dozens of interacting proteins and responds to both developmental and environmental cues (Lloyd, 1991). Actin is a major component of the plant cytoskeleton and is thought to be required for correct cell-division plate alignment and synthesis, cell-shape determination, cell-polarity establishment, cytoplasmic streaming, organelle movement, and tip growth (Staiger and Schliwa, 1987; Staiger and Lloyd, 1991; Meagher and Williamson, 1994). These processes are of central importance in plant development; however, we know very little about how plant actin microfilament ar-

rays are regulated or how they interact with other cytoskeletal components.

Plants contain multiple actin isoforms encoded by large, ancient gene families (Meagher and McLean, 1990; Meagher, 1991). The actin gene families of petunia (Baird and Meagher, 1987), soybean (Nagao et al., 1981; Hightower and Meagher, 1985), tobacco (Thangavelu et al., 1993), potato (Drouin and Dover, 1990), and rice (McElroy et al., 1990) contain dozens or even hundreds of actin sequences. Hightower and Meagher (1986) demonstrated that the soybean actin gene family contains ancient actin gene subclasses that arose early in land-plant evolution. They proposed that these subclasses have been conserved during vascular plant evolution because they have advantageous expression patterns or encode actin isoforms with unique functions. Studies demonstrating the functional importance of plant actin gene multiplicity, differential expression, and protein isoform diversity have been complicated by the large gene families encoding actin in most plant species (Meagher and Williamson, 1995).

We are using Arabidopsis thaliana as a model to investigate the regulation and functions of ancient plant actin subclasses. By linking the genetic regulation of plant actins with their specific subcellular functions, we hope to expand our understanding of the cytoskeleton's role in plant development. Arabidopsis contains a relatively simple actin gene family of 10 members that can be grouped into two ancient classes and further grouped into six ancient subclasses (Nairn et al., 1988; McDowell et al., 1996). The ancient Arabidopsis actin subclasses have not shared common ancestral sequences for several hundred million years, and the subclasses of protein are far more divergent in charged residue substitutions than are all of the actins in the animal kingdom.

This paper describes the expression of the Arabidopsis ACT7 actin gene, which is the sole representative of one distinct subclass. ACT7 is preferentially expressed in vegetative tissues that contain rapidly dividing and expanding cells and appears to be the only actin expressed in the hypocotyl and seed coat. In addition, ACT7 was differentially regulated in response to exogenous hormone treatment. Although the gene tree groups ACT7 in a class with

¹ This work was supported by a grant from the National Institutes of Health to R.B.M. J.M.M. was supported by a National Institutes of Health predoctoral training grant fellowship in genetics. This work serves a partial fulfillment of the requirements for a Ph.D. in genetics for J.M.M.

* Corresponding author; e-mail meagher@bscr.uga.edu; fax 1-706-542-3910.

Abbreviations: ABRE, ABA response elements; GARE, GA₃ response elements; IPA, N-6-(δ -2-isopentyl) adenine; nt, nucleotide; RT-PCR, reverse-transcriptase mediated PCR.

a second subclass of vegetative actins, the patterns of *ACT7* expression are completely distinct from the other seven expressed *Arabidopsis* actins. We discuss the evidence that *ACT7* is a distinct and possibly indispensable member of the *Arabidopsis* actin gene family.

MATERIALS AND METHODS

Gene Isolation, Sequence Determination, and Primer Extensions

ACT7 was initially isolated as two independent cDNAs from an *Arabidopsis thaliana* root λ gt11 library (kindly provided by Brian Hauge and Howard Goodman, Massachusetts General Hospital, Boston). An *ACT7*-specific hybridization probe was prepared by amplifying a 3' flanking sequence from the last *ACT7* codon (codon 377) to 233 bp downstream of the stop codon by the PCR (McDowell et al., 1996). This probe was used to isolate an *ACT7* genomic clone, λ ACT7, from a λ GEM11 library of randomly sheared *cv* Columbia DNA (generously provided by John Mulligan and Ron Davis, Stanford University, Stanford, CA). A 4.0-kb genomic *Hind*III fragment containing the *ACT7* coding sequence and the 5' flanking sequence was subcloned into pBluescript SK+ to create pACT7H. The *ACT7* transcription start site was determined by primer extension on total RNA made from the above-ground portions of 3-week-old plants as described previously (An et al., 1996). The antisense primer ACT7-5'NP was complementary to the RNA sequence from -589 to -570 nt upstream from the start site. The DNA sequence of the genomic clone was determined using the same primer and run in parallel as a standard.

DNA Gel Blots

Genomic DNA was isolated from *Arabidopsis cv* Columbia by a method described previously (McLean et al., 1988). The DNA was digested and fractionated in a 0.8% agarose gel at 40 V for 16 h. The DNA was then transferred to a nylon membrane (Biotrans Plus, ICN) in a Transvac vacuum blotter (Hoefer Scientific Instruments, San Francisco, CA) according to the manufacturer's instructions, and it was fixed to the membrane by 3 min of UV irradiation and 2 h of baking at 80°C. The 1.8-kb PCR fragment that contained the 5' flanking sequences as described above was labeled by the random primer method (Feinberg and Vogelstein, 1983) to a specific activity of approximately 0.5×10^9 cpm/ μ g. The probe was hybridized to the blot in $6 \times$ SSC, $5 \times$ Denhardt's solution, 0.2% SDS, and 40% formamide at 56°C for 48 h. The blot was washed four times for 10 min each at 56°C in $0.5 \times$ SSC, 0.2% SDS and exposed to x-ray film (X-Omat, Kodak) with one intensifying screen for 48 h at -70°C. The specificity of the 5' probe for *ACT7* was confirmed by hybridizing it to dot blots of the nine other *Arabidopsis* actin genes (McDowell et al., 1996). No cross-hybridization was observed.

RNA Preparation and Northern Analysis

Roots, stems, and leaves of 3-week-old plants, flowers (approximately 90% unopened) and siliques of 5- to

6-week-old plants, and intact 6-d-old seedlings were collected into liquid nitrogen and stored at -70°C before use. Total RNA was prepared from these tissues essentially by the method of Logemann et al. (1987). Pollen RNA was prepared as described (S. Huang, Y.-q. An, J. McDowell, E.C. McKinney, R.B. Meagher, unpublished data). Five micrograms of total RNA from each of the tissues was fractionated in a 1% agarose/formaldehyde gel (Sambrook et al., 1989) and blotted to a nylon membrane (4.5 μ m, Biotrans+, ICN) for 20 h. The filters were prehybridized overnight in $1 \times$ RNA hybridization mixture (Thompson et al., 1992) containing 40% formamide at 48°C. The 3' flanking sequence of *ACT7* was utilized as a gene-specific hybridization probe for the *ACT7* mRNA. Hybridization was carried out for 24 to 30 h in the conditions described above with approximately 3×10^6 cpm/mL of the probe labeled at approximately 6×10^8 cpm/ μ g DNA by the random primer method of Feinberg and Vogelstein (1983). Filters were washed once for 15 min at 48°C in $2 \times$ SSC/0.2% SDS and twice for 15 min at 48°C in $1 \times$ SSC/0.2% SDS. After a brief drying period, the filters were exposed to x-ray film (Kodak) with two intensifying screens at -70°C for 1 to 3 d. Gene-specific hybridization was confirmed by including DNA blots of closely related actin genes (*ACT2* and *ACT11*) (McDowell et al., 1996) in the hybridization. No cross-hybridization was detected (data not shown). Equal loading of the RNA samples was confirmed by rRNA hybridization. The northern blots were stripped and rehybridized with a 26-nt 18S rRNA oligonucleotide (Tanzer and Meagher, 1994). The hybridization was performed at 48°C for 20 h with approximately 1×10^7 cpm of the probe labeled at approximately 1×10^6 cpm/pmol oligonucleotide. Washes were conducted three times for 15 min at 48°C in $2 \times$ SSC/0.5% SDS. After a brief drying period, the filters were exposed to x-ray film for 30 min with two intensifying screens.

RT-PCR

Samples of total RNA (5 μ g) from seedling, root, stem, leaf, flower, pollen, and silique were reverse transcribed into cDNA. Forty picomoles of oligo(dT) were used in 50- μ L reactions with 8 units of avian myeloblastosis virus reverse transcriptase (Promega) in the manufacturer's recommended buffer. The level of cDNA synthesis was measured by assaying DNA concentration with Hoechst dye in a DNA mini-fluorometer (Hoefer Scientific Instruments) following the manufacturer's instructions. The total yield typically ranged from 200 to 300 ng. For PCR amplification of each cDNA sample, a series of 12 2-fold serial dilutions was constructed. The first sample in each series contained 2 ng of cDNA. Each 50- μ L PCR reaction contained 0.1 mM deoxyribonucleotide triphosphate, 25 pmol of each primer, 2.5 μ g of linear acrylamide carrier, 50 mM KCl, 10 mM Tris-HCl, pH 8.8, 1.5 mM MgCl₂, and 0.1% Triton X-100 (Sigma). The linear acrylamide was polymerized for 30 min at room temperature in a 50-mL solution of 40 mM Tris-HCl, pH 7.5, 20 mM NaOAc, 2 mM EGTA by adding 0.5 mL of 10% ammonium persulfate and 50 μ L of *N,N,N',N'*-tetramethylethylenediamine (Eastman Kodak). One gen-

eral actin oligonucleotide in the third coding exon (ACT327S) and one gene-specific oligonucleotide in the fourth coding exon near the end of the 3'UTR (ACT7-3'N2) were used to amplify the 3' end of the ACT7 transcript. The reaction was subjected to 45 cycles at 94°C (1 min), 42°C (1 min), and 72°C (30 s). One-fifth of each PCR reaction was run in each lane of an agarose gel and stained with ethidium bromide, and samples from different organ amplifications were run on the same gel for comparison. Approximations of relative RNA levels in each sample were based on the first dilution in each series in which a product was not visible.

GUS Fusion Constructs

The 1.8-kb ACT7 5' region was amplified by PCR from pACT7 with the T3-17 and PLAc12N-Bam oligonucleotides (Table I; Fig. 1A). The fragment was digested with *Hind*III and *Bam*HI and ligated into binary vector pBI101.1 (Clontech, Palo Alto, CA). The actin sequence was inserted in frame with the GUS coding sequence 24 bp downstream of the GUS translation initiation codon. This construct produced an ACT7/GUS fusion protein fully capable of cleaving 5-bromo-4-chloro-3-indoyl- β -D-glucuronic acid. Two constructs were created from independent amplifications of the ACT7 5' flanking region (pACT7 h1 and pACT7 h2). The constructs were transformed into *Agrobacterium* strain LBA4404 by the method of An et al. (1988). These strains were utilized to transform Arabidopsis cv RLD according to a variation of Marton and Browse (1991) as described (An et al., 1996). Primary transformants were screened for GUS activity. T₂- and T₃-generation plants from several independent transformations with each construct were subjected to detailed histochemical analysis. The expression patterns of the two constructs were essentially identical, indicating that any mutations that might have occurred during the amplification did not affect promoter function.

Table I. Oligonucleotide primers

Sequences are listed 5' to 3'. The underlined segments are restriction sites and clamps. The T3-17 primer anneals to the T3 promoter in pBluescript. Oligonucleotides prefaced with ACT7 anneal to ACT7 only, and not to other actin genes. The remaining oligonucleotides are degenerate and hybridize to all Arabidopsis actin sequences. N = A or G or C or T; R = A or G; W = A or T; Y = C or T; D = A or G or T. The numbers refer to the N-terminal codon in the sequence, except for ACT7-3'N1 and ACT7-3'N2, which anneal 255 and 233 bp downstream of the ACT7 stop codon, respectively, and ACT7-5'NP, which anneals 585 bp upstream of the first ATG (Fig. 1A). S or N in the "Name" column designates that the sequence is identical to the sense or nonsense strand of the gene, respectively.

Name	Sequence
T3-17	ATTAACCTCACTAAAG
ACT7-5'NP	AGAAGATTCGAGAAGCAGCG
ACT7-376S	AGCTCCCGGGCTAAGTGTGTCTTGTCTTATCTGGT
ACT7-3'N1	AGCTCCCGGGGACTAAACCAGGAAACCAATATAA
ACT7-3'N2	TGAACCAAGGACCAATATAATATG
PLAc12N-Bam	CGCACGGATCCTACCATNCCNGTNCRRTRTRCRA
ACT119S	GARAARATGACNCARATNATGTTYGA
ACT284N	ATRTCACRTRCAYTTCATDAT
ACT327S	ATGAARATNAARGTNGTNGCNCNCNCA

Assay for GUS Activity

Plant tissue was fixed in 90% acetone for 1 h, followed by two equilibrations in 50 mM sodium phosphate, pH 7.0, for 30 min each (Hemerly et al., 1993). The acetone fixation slightly coagulated soluble protein and extracted membrane lipids, thereby facilitating substrate penetration. The tissue was then stained histochemically in 0.5 mM 5-bromo-4-chloro-3-indoyl- β -D-glucuronic acid, 0.5 mM K₃[Fe(CN)₆], 0.5 mM K₄[Fe(CN)₆], 0.1% Triton X-100 for 5 or 24 h at 37°C (Jefferson et al., 1987). Chlorophyll was then extracted with 70% ethanol. Data were recorded on a Zeiss compound microscope or a Wild (Heerbrugg, Switzerland) dissecting scope with Kodak Ektachrome 64T film. Quantitative GUS assays were performed according to the method of Jefferson et al. (1987). Protein concentrations were measured according to the method of Bradford (1976).

Hormone Treatment and Plant Growth

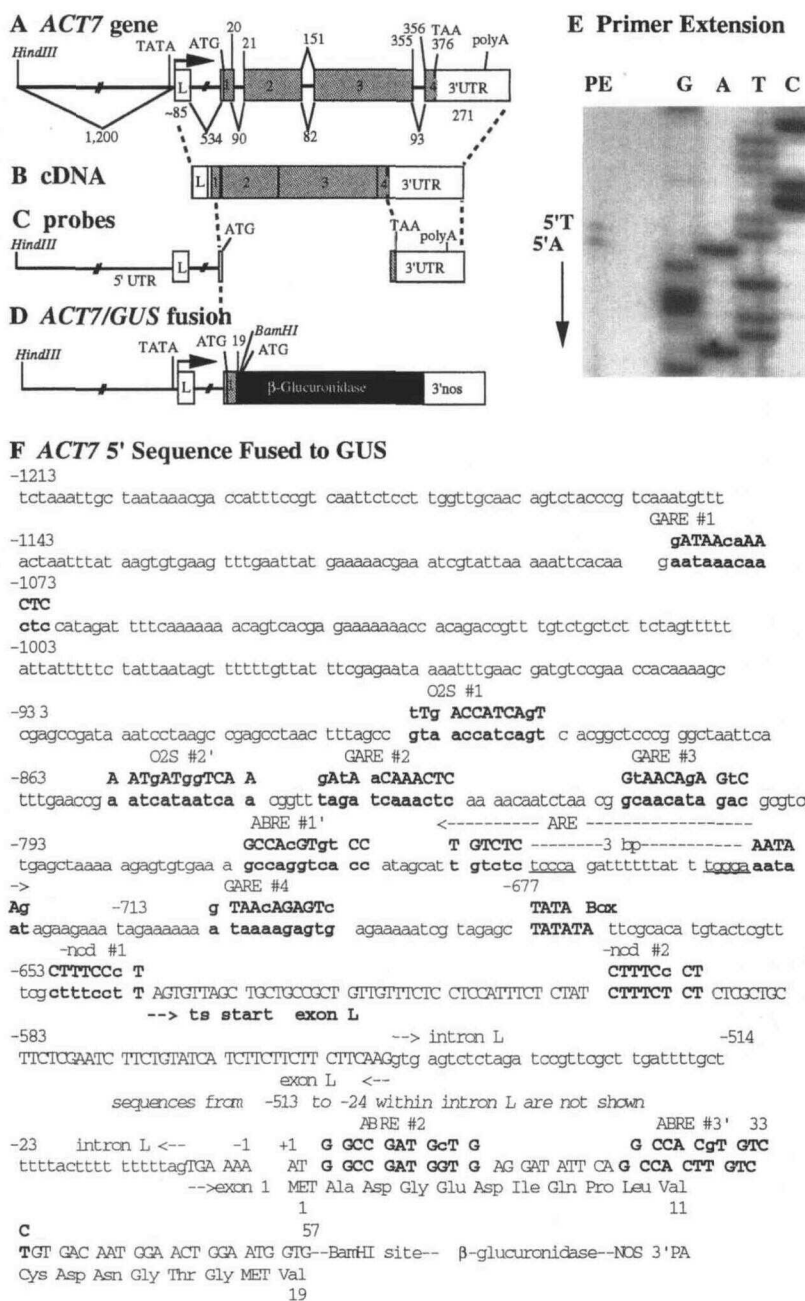
T₃ plants from three different transgenic lines were grown on normal Murashige and Skoog salts medium (Life Technologies) for 28 d at 22°C with 12 h of light per day, and then shifted to soft agar (0.3% phytagar, GIBCO-BRL) Murashige and Skoog salts medium supplemented with one of the following hormones at the concentration indicated: 0.1 μ M 2,4-D, 1 μ M IAA, 10 μ M IPA, 10 μ M GA₃, 10 μ M ABA, and 1 μ M hydroxyurea. The hormones were purchased from Sigma. Plants were histochemically stained for GUS expression after 24 and 48 h.

RESULTS

Structure of the ACT7 5' Region

ACT7 cDNA and genomic clones were isolated, and the coding sequence was determined as described in "Materials and Methods." A quantity (1210 bp of nt sequence upstream of the initiator ATG and 697 bp downstream of the stop codon) was also determined from the genomic clone. Comparison of the genomic and cDNA sequences shown in Figure 1, A and B, respectively, revealed that three small introns split the ACT7 coding sequence between codons 20 and 21, within codon 151, and between codons 355 and 356, and that a 537-bp intron interrupted the 5' untranslated region at a position 6 nt upstream of the first ATG (Fig. 1A). This intron in the mRNA leader will be referred to as intron L, and the upstream exon will be referred to as exon L. The ACT7 cDNA sequence, in combination with mapping of the transcription start sites by primer extension analysis as shown in Figure 1E, also revealed that the ACT7 mRNA contained 101 to 102 nt of sequence upstream of the first actin ATG. The two ACT7 transcription start sites, 5' T and 5' A (Fig. 1, E and F), were positioned 643 and 642 bp upstream of the initiator ATG and were 33 and 34 bp downstream of the first A in a putative TATA box (TATATA) (Fig. 1, A and F). The ACT7 message was polyadenylated 271 nt downstream of the stop codon (Fig. 1B) as inferred from the cDNA sequence.

Figure 1. Physical maps of the *ACT7* gene and cDNA, DNA probes, and the *ACT7/GUS* fusion. A, Map of *ACT7* gene structure in pACT7H. The lengths of the 5' flanking sequence, the leader exon, the introns, and the 3' untranslated region (3'UTR) are indicated below the map. Transcribed regions are indicated on the map by open boxes. Translated regions are shaded. L, 3.4 kb. B, A physical map of the independently cloned and characterized *ACT7* cDNA. L, 1.5 kb. C, DNA probes from the 5' and 3' untranslated regions (5'UTR and 3'UTR; 1.8 and 0.3 kb, respectively). D, Map of the *ACT7/GUS* fusion construct in pBI101.1. E, Primer extension mapping of the 5' end of the *ACT7* transcript. Two reverse-transcriptase stop sites at the 5' end of the mRNA were identified as T and A residues, 102 and 101 nt upstream of the first nucleotide in the ATG initiation codon and 33 and 34 bp downstream of the first **A** in a putative TATA box, respectively (see F). Although the sequence of the antisense cDNA and antisense genomic DNA control strand were determined in this experiment, the bands are labeled with the complementary sequence of the sense strands so that the data are easily correlated with the sequence of the 5' end of the mRNA transcript. F, DNA sequence of a portion of the 5' region from *ACT7*, which was fused to GUS reporter and nopaline synthase 3' polyadenylation signals (NOS 3'PA). Exons and the TATA box, which is thought to specify the start of transcription, are shown in uppercase, and introns and flanking sequences are shown in lowercase. Previously identified phytohormone responsive motifs (boldface) are shown above the *ACT7* sequence (see "Discussion" for the references to these sequence elements). Most of intron L in the mRNA leader has been deleted from the figure to save space. ts start, -642 and -641; TATA box, -677 to -672; intron L, -546 to -7; GARE #1, -1082 to -1071; GARE #2, -837 to -826; GARE #3, -811 to -801; GARE #4, -704 to -694; O2S #1, -896 to -885; O2S #2, -854 to -843; ABRE #1, -772 to -761; ABRE #2, +3 to +13; ABRE #3, +24 to +34; ARE, -753 to -722; nod #1, -650 to -642; and nod #2, -899 to -892.



It was not determined if additional poly(A) addition sites exist.

To determine if Arabidopsis contained any other actin genes that were very closely related to *ACT7*, a 1.8-kb *ACT7* 5' flanking sequence probe (Fig. 1C, 5' UTR) was hybridized at moderate stringency to a gel blot of Arabidopsis genomic DNA. The *ACT7* 5' probe did not cross-hybridize to any of the other nine Arabidopsis actin genes we have isolated (data not shown). This probe should have detected any closely related sequences (>70% nucleic acid identity) under the hybridization conditions used (Hightower and Meagher, 1985). Figure 2 shows that the *ACT7* probe hybridized strongly to one or two bands in each of five

restriction enzyme digests. The two bands in the *EcoRI*, *BglIII*, and *HincII* digests resulted from cleavages in the *ACT7* 5' region, as determined from the sequence of the 5' region. These and other data (McDowell et al., 1996) suggested that there are no other actin gene sequences in the Arabidopsis genome having a high degree of identity and recent ancestry with *ACT7*. A complete phylogenetic analysis of the *ACT7* sequence compared with the other nine Arabidopsis actin genes confirms these data, suggesting that *ACT7* represents one of six distinct, evolutionarily ancient subclasses of actin that may predate the separation of monocots from dicots 200 million years ago (McDowell et al., 1996).

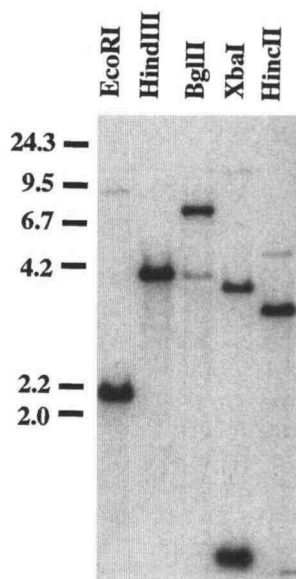


Figure 2. Arabidopsis DNA blot hybridized with an *ACT7* 5' flanking sequence probe. Five micrograms of Arabidopsis DNA were digested with the indicated enzyme, separated on a 0.8% agarose gel, and transferred to a nylon membrane. A 1.8-kb gene-specific probe from the 5' region of *ACT7* was hybridized to the blot under moderate stringency.

ACT7 mRNA Abundance

The steady-state level of *ACT7* mRNA was examined in different organs and tissues with RNA gel blots and RT-PCR. RNA was isolated from roots, stems, leaves, flowers, pollen, and green siliques. A gel blot of these RNA samples was probed with a 270-bp segment of *ACT7* 3' flanking sequence (Fig. 1C, 3'UTR), which hybridizes specifically to the *ACT7* sequences and not to the other nine actin genes (Fig. 3C). A 1.5-kb *ACT7* transcript was detectable in all of the samples except pollen, as shown in Figure 3A. The intensity of hybridizing bands indicated that *ACT7* mRNA was most abundant in the inflorescence stem, followed by flowers, and then leaves. Roots and siliques contained the lower levels of *ACT7* mRNA, and RNA was not detected in pollen. Rehybridization of the filter with an 18S rRNA probe demonstrated that equal amounts of total RNA were loaded on the gel and transferred to the blot (Fig. 3B).

The results from the northern blot analysis were corroborated by RT-PCR with *ACT7*-specific amplification primers that spanned intron 3, exon 4, and the 3' untranslated region in the *ACT7* message (Fig. 1A; Table I). cDNA from 6-d-old seedlings was included in the analysis along with cDNA from the tissues and organs that were analyzed on the northern blot. A series of 2-fold dilutions, which began with an equal amount of input cDNA from each sample, was amplified. Figure 4 demonstrates that *ACT7* mRNA was present in all of the samples, including pollen. We inferred the relative levels of *ACT7* message in each of the tissues, based on the first dilution point in each series at which no amplification product was visible in agarose gels. Overall, there was an approximately 128-fold variation in the relative levels of *ACT7* mRNA among the different

organs and tissues. As seen on the northern blot, the highest levels of *ACT7* message were observed in inflorescence stems, followed by flowers, seedlings, leaves, siliques, roots, and finally pollen. The relative levels of *ACT7* mRNA determined from the dilution end points were: inflorescence stems, 128×; flowers, 32×; leaves, 16×; siliques, 16×; seedlings, 16×; roots, 8 to 16×; and pollen, 1× (see "Materials and Methods"). These results were reproducible in amplifications of two independent cDNA preparations from each tissue. Pollen expression was so weak that a PCR product was barely visible even at the highest cDNA input levels. Our inability to detect *ACT7* mRNA in pollen on the northern blot undoubtedly reflects the lower sensitivity of the gel blot hybridization technique relative to RT-PCR.

Differential Regulation of *ACT7/GUS* Expression during Arabidopsis Development

The organ-level differences in *ACT7* mRNA abundance suggested that *ACT7* was differentially regulated. To examine *ACT7* transcriptional regulation at the level of tissues and cell types, we constructed a fusion between 1.9 kb of 5' sequence from *ACT7* and the *GUS* reporter gene and monitored the expression of this construct in transgenic Arabidopsis plants. The construct contained 1.2 kb of *ACT7* sequence upstream of the transcription start site, the leader exon, the leader intron, and the first 19 codons of *ACT7* coding sequence fused in translational frame with *GUS* (Fig. 1D). Exon L, intron L, and the 5' coding sequence were included in the construct, because previous studies suggested that they might contain important regulatory elements (Pearson and Meagher, 1990;

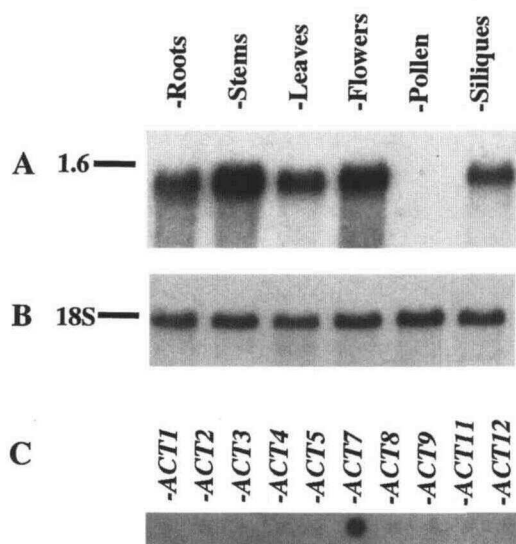


Figure 3. Arabidopsis RNA blot hybridized with an *ACT7*-specific 3' flanking sequence probe. A, Hybridization with a gene-specific probe from the *ACT7* 3'UTR. A single transcript of approximately 1500 nt was detected at varying levels in each of the organ RNA samples but not in pollen. B, Hybridization of the same blot with a 26S rRNA probe demonstrates equal loading in all lanes. C, Control hybridization of the *ACT7*-specific 3' probe hybridized to a blot of 10-ng samples of plasmid DNA clones for the 10 Arabidopsis actin genes.

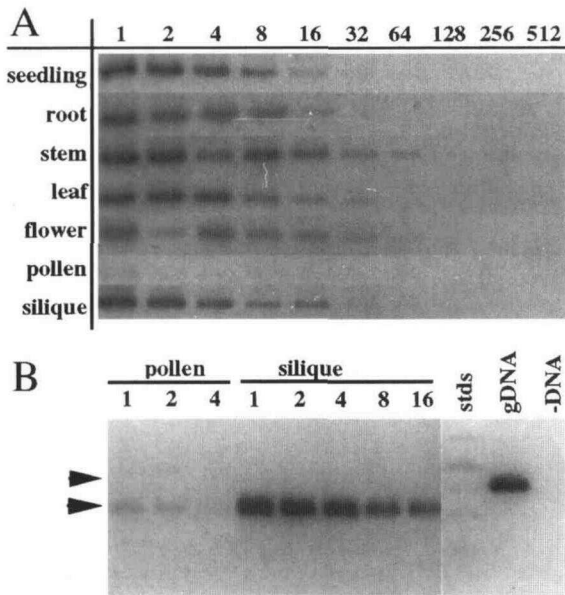


Figure 4. RT-PCR of *ACT7* mRNA. A, Reverse transcriptase and oligo(dT) were used to generate cDNA from seedling, root, stem, leaf, flower, pollen, and silique RNA samples. An approximately 400-bp fragment of *ACT7* cDNA was amplified from the end of the protein coding region (codon 327) through most of the 3'UTR, to near the polyadenylation site with the ACT327S and ACT7-3'N1 oligonucleotide primers (Table I). The first sample (lane 1) in each series contains 2 ng of cDNA, and the other samples represent a 2-fold dilution series (e.g. lane 2 contains 0.5× starting template than lane 1, lane 4 contains 0.25× starting template, etc.). One-fifth of each reaction was resolved on a 1.5% agarose gel and stained with ethidium bromide. The figure presents the negative of the fluorescent image. B, Reproducibility of the relative levels of RT-PCR products. An independent experiment was performed on independently prepared RNA samples from the same organs and tissues as in A. The products from pollen RNA are shown relative to silique RNA as a control (black arrowhead). Also indicated are the sizes of the products generated from genomic DNA (gDNA, gray arrowhead), which contains an intron in the region amplified, a control reaction in which the DNA template was omitted (-DNA), and DNA size standards (stds) composed of pBR322 digested with *A*lul.

Zhang et al., 1991). Transgenic *Arabidopsis* plants were generated by *Agrobacterium*-mediated transformation, and T₂ and T₃ plants from 17 independently transformed lines were assayed for GUS activity at several stages in their life cycles. Tissue was treated with acetone prior to staining to enhance substrate penetration (Hemerly et al., 1993). Seven of the transgenic lines contained the *pACT7 h1* fusion, and 10 contained the *pACT7 h2* fusion, which were both prepared from independent PCR amplifications of the 5' region. Approximately 1 kb of 5' flanking sequence was determined on each construct; in *pACT7 h1*, five 1-bp substitutions and one 1-bp deletion were discovered, whereas *pACT7 h2* contained no mutations in this region (data not shown). The spatial patterns of GUS expression shown in Figure 5 were comparable in all of the plant lines examined, so we will make no additional distinction between the *pACT7 h1* and *pACT7 h2* constructs and will refer to them collectively as *ACT7/GUS*. Some of these data are summarized in Table II. Variations in the

intensity of staining within and between the progeny of different transformants were occasionally observed. This phenomenon has been frequently described and is usually attributed to the copy number of the transgene, the chromosomal position of the construct, and/or physiological variations among the plants. No endogenous GUS activity was observed in untransformed control plants (data not shown).

Seedlings

Strong histochemical GUS staining was observed in the aleurone layer of the seed (Fig. 5A). This activity was detectable during the first 3 d after germination, but was not observed in seeds that were stained 7 to 10 d after germination. GUS staining was weak in most seedling tissues a few hours after imbibition, but was expressed strongly in all tissues in 3- to 7-d-old seedlings. As seen at the top of Figure 5B, GUS was expressed throughout the cotyledon, hypocotyl, and root of 7-d-old seedlings. The highest level of GUS activity was found in the root, based on the staining intensity and the time at which staining was first visible. Examination of tissue sections indicated that GUS was expressed in all seedling cell types (data not shown). After 10 d of growth, GUS activity remained high in the cotyledons and root, but was low or undetectable in the hypocotyl (Fig. 5B, bottom). In etiolated seedlings, however, strong GUS activity persisted in the hypocotyl even after 11 d (Fig. 5B, middle). This activity was usually confined to the top half of the hypocotyl. These data suggest a link between *ACT7* expression and cell elongation. Dynamic changes in the actin cytoskeleton are thought to be central to plant cell elongation (Seagull et al., 1987; Seagull, 1989).

Juvenile Plants

Strong GUS activity was consistently exhibited in emerging leaves and roots during rosette development. For example, Figure 5C shows that primordia of the first two true leaves exhibited strong, uniform GUS activity. As the petiole and blade expanded, the pattern of GUS expression changed: the highest levels of GUS expression were observed in trichomes and small, circular patches of cells in the leaf (Fig. 5D). GUS staining was particularly intense in trichomes. The small, circular areas of staining were concentrated around stomata and groups of mesophyll cells underneath stomata. *ACT7* may be involved in the unique cytoskeletal arrays that form in trichomes and stomata during differentiation (Brown and Lemmon, 1985; Parthasarathy et al., 1985; Cho and Wick, 1991). GUS activity was very low in the epidermal and cortical tissues of the petiole, but was generally high in the vascular tissue. As the leaf matured and expanded, GUS staining became weaker and more uniform throughout the leaf blade (Fig. 5E). In fully expanded leaves in older rosettes, GUS staining was noticeably weaker and often barely detectable (Fig. 5F).

Figure 6 shows the results from a quantitative comparison of GUS activity in developing leaves and fully expanded leaves (see "Materials and Methods"). Using 35-d-old plants with rosettes of 7 to 10 leaves, GUS activity from

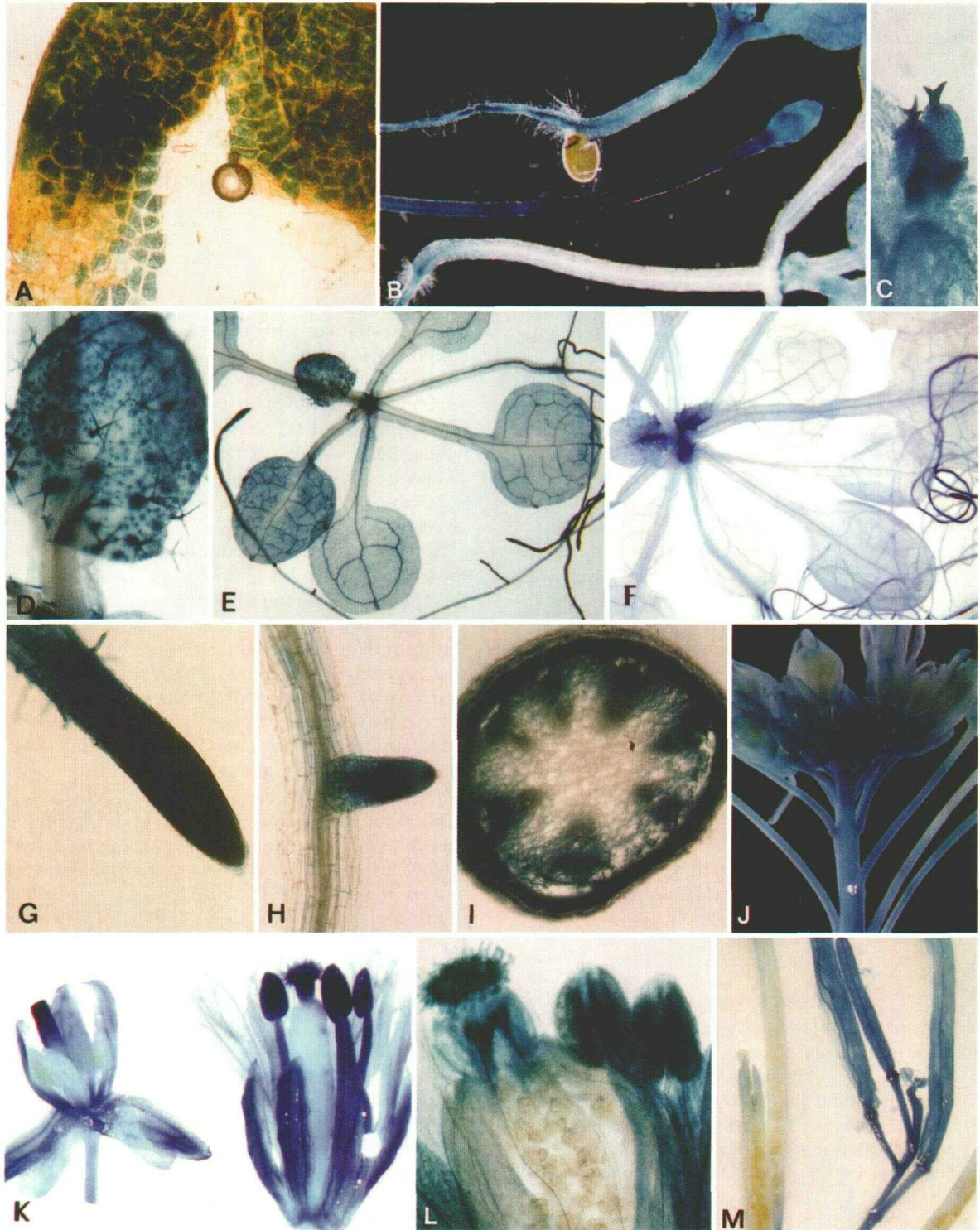


Figure 5. Histochemical localization of *ACT7/GUS* expression in transgenic *Arabidopsis* plants. These data for 17 independent transgenic lines are summarized in Table I. A, Seed coat showing staining in the aleurone layer. B, Seedlings. Top, 7-d-old, light grown; middle, 11-d-old, etiolated; bottom, 11-d-old, light grown. C, Leaf primordia from a 7-d-old plant. D, Expanding leaf from a 3-week-old plant. E, Three-week-old plant. F, Six-week-old plant. G, Apex of a primary root in a 3-week-old plant. H, Lateral root primordium arising from fully differentiated root tissue in a 3-week-old plant. I, Cross-section of inflorescence stem. J, Inflorescence. K, Stage-13 (left) and -14 (right) flowers. L, Anthers and top of carpel from a stage-14 flower. M, Maturing siliques.

Table II. Organ-level expression of 5' *ACT7/GUS* in progeny of independently transformed plants

SC, Alurone layer of seed coat; Se, all seedling cell types; YL, young leaf; ML, mature leaf; YR, young root tissue; MR, mature root tissue; P, S, petal and sepal; Pi, Pistil; St, stamen; Po, pollen; IS, inflorescence stem; Si, silique; Em, embryo.

Plant Lines	Seedling		Juvenile Plant				Inflorescence						
	SC	Se	YL	ML	YR	MR	P, S	St	Pi	Po	IS	Si	Em
Expressing	17	17	17	0 ^a	17	0 ^a	17	17	16	15	17	16	0
Examined	17	17	17	17	17	17	17	17	17	17	17	17	17

^a Expression in these tissues was dramatically lowered or undetectable.

the first 2 true leaves, which were now fully expanded, was compared with that of the 3 youngest leaves, including 1 expanding leaf of approximately 1 mm width. Three independent plant lines were assayed that showed a significant reduction in GUS specific activity in mature leaves. The reduction in GUS activity ranged from 30% to 4-fold in the three plant lines. This experiment confirmed that the decrease in staining intensity in older leaves represented a bona fide down-regulation of *ACT7/GUS* expression and not simply a dilution of the dye precipitate in the larger, vacuolated cells of mature leaves.

ACT7/GUS was also developmentally regulated in the roots of juvenile plants. At the root apex (Fig. 5G), GUS was expressed throughout the meristematic zone, the zone of elongation, and the zone of differentiation (Schiefelbein and Benfey, 1991) at high levels. In mature portions of the root, the pattern of GUS expression became progressively restricted. Activity generally declined in the epidermis first, followed by the cortex, and then the vascular cylinder. The expression in vascular tissues might reflect the relatively late and protracted differentiation that occurs during secondary wall thickening (Dolan et al., 1993). In fully differentiated root tissue, GUS activity was detectable only in the endodermis and/or the pericycle (Fig. 5H). However, *ACT7/GUS* was fully reactivated in lateral root primordia (Fig. 5H); as lateral roots developed, the expression pattern described above was repeated.

Inflorescence and Flowers

ACT7/GUS was also differentially expressed in the floral organ complex. GUS was strongly expressed in young inflorescence stem tissue (Fig. 5J). As seen in Figure 5I, the construct was expressed throughout the stem, except in the pith. No GUS activity was observed in older regions of the stem, except around wound sites (not shown). In immature flowers, GUS activity was observed in the sepals and the petals (Fig. 5, J and K). This activity decreased or disappeared as the sepals and petals stopped expanding. GUS activity was also observed in developing pistils of all lines. Eleven of the 17 transformed lines still expressed GUS throughout most or all of the carpel wall, the transmitting tract, and the stigmatic papillae in elongating carpels. In 5 of the remaining 6 lines, GUS activity was detected only in the upper half of the elongating carpel. Fully mature carpels usually exhibited little or no GUS activity, although 12 of the 17 lines exhibited GUS activity in the stigmatic papillae. No GUS activity was ever detected in the ovules at

any stage of carpel development, even in carpels that had been cut to allow substrate penetration (Fig. 5L).

The most striking regulation of *ACT7/GUS* in flowers occurred in the stamen. As seen in Figure 5, J and K left, little or no GUS expression was observed in the stamen through stage 13 (Smyth et al., 1990) of flower development. By stage 14, however, strong GUS activity was observed in the filament, anther, and pollen (Fig. 5, K right and L). However, in 2 of the 17 lines examined, no pollen expression was observed, which is in closer agreement with the data on steady-state RNA levels (see "Discussion").

In the silique, GUS activity was consistently observed at the base. In 13 of the 17 lines, GUS was also expressed at the apex of the silique. In 4 of the 17 transgenic lines, the GUS gene was reactivated in the wall of the pistil after fertilization and remained active in the wall during seed-pod development (Fig. 5M). GUS activity was not observed in ovules or embryos at any stage of silique development, even in ovules from siliques that had been cut to facilitate substrate penetration. Cut, dried seeds did show low to moderate activity in all tissues of the embryo. It is interesting that the different plants we analyzed displayed more variation in the intensity and pattern of GUS expression in the floral organs and siliques than in any other organs, although the spatial features reported above were consistent among the majority of the plants. It is possible that the regulation of *ACT7* in the inflorescence is influenced by unknown environmental or physiological factors.

Effect of Exogenous Phytohormones on *ACT7/GUS* Expression

The preferential expression of *ACT7/GUS* in proliferating tissues suggested that *ACT7* expression could be influenced by plant growth regulators. To test this possibility, T₃ plants from three different transgenic lines were grown on normal medium for 28 d and then shifted to medium supplemented with the auxin 2,4-D, IAA, the cytokinin IPA, GA₃, ABA, or hydroxyurea, which inhibits cell division (Hemerly et al., 1993). Plants were histochemically stained for GUS expression after 24 and 48 h. Little effect on the intensity or pattern of GUS expression in aerial parts of the plant was observed in any of the treatments. Control plants that were not exposed to phytohormones exhibited the normal pattern of ubiquitous *ACT7/GUS* activity as described above and as shown in Figure 7A.

The roots of plants treated with three classes of phytohormones—cytokinins, ABA, and auxins—displayed striking spatial alterations in GUS activity correlating with re-

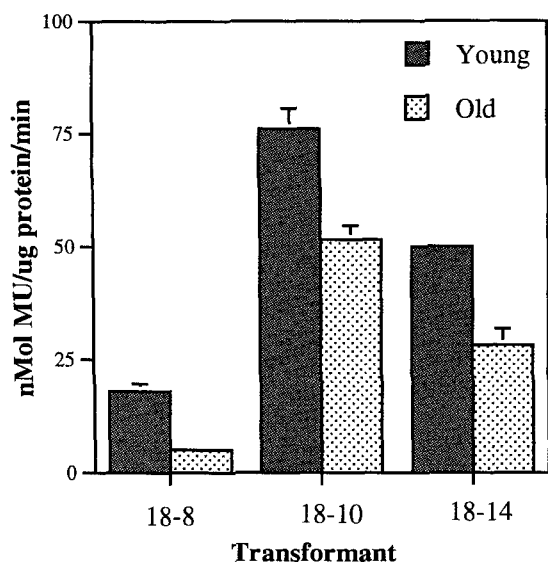


Figure 6. Quantitative comparison of *ACT7/GUS* activity in expanding and mature leaves. The 3 youngest leaves, including 1 expanding leaf of approximately 1 mm width (young leaves) and the first 2 true leaves, which were now fully expanded (old leaves), were removed from 35-d-old plants with rosettes of 7 to 10 leaves. The levels of GUS activity are displayed as nanomoles methylumbelliferone (MU) produced per minute, normalized to milligrams of total cellular protein. Three T_3 plants from 3 independent transformed lines were assayed in each experiment. GUS expression in the young leaves is represented by solid bars, and GUS levels in mature leaves are denoted by dotted bars. Each value is the average of 2 to 3 independent experiments, with the SE indicated by the error bar.

gions of rapid growth when compared to untreated control plants. These changes were most apparent after 48 h of hormone treatment, and representative results are shown in Figure 7. Treatment with the cytokinin IPA noticeably restricted the pattern of *ACT7/GUS* expression at the root apex (Fig. 7B). Strong GUS activity was present only in the meristematic zone, the lower part of the elongation zone, and the vascular cylinder. GUS activity was very low or undetectable in the epidermis and cortex. In addition, GUS activity in the vascular cylinder of cytokinin-treated roots disappeared much more quickly in progressively more mature tissues than it did in untreated roots. ABA treatment also altered *ACT7/GUS* expression, but in a different pattern from cytokinin treatment (Fig. 7C). GUS activity was completely abolished in most of the meristematic zone, but its pattern in the elongation zone resembled that of untreated roots. Above the elongation zone, however, GUS activity disappeared very quickly as the root matured, as was seen in cytokinin-treated roots. Auxin treatments produced obvious root morphology changes that were accompanied by alterations in *ACT7/GUS* expression. Treatment with the synthetic auxin 2,4-D broadened the root apex and caused a proliferation of abnormally long root hairs very close to the root apex (Fig. 7D). 2,4-D also stimulated the initiation of lateral root, primordia-like outgrowths along the length of the root. *ACT7/GUS* was expressed at the very tip of the root; in some root hairs in the apex, in the vascular cylinder, and in lateral root primordia. IAA treat-

ments (Fig. 7E) did not affect root apex morphology as dramatically as 2,4-D at the concentrations we used, but they did cause a proliferation of root-primordia-like structures, as was seen in 2,4-D-treated plants. *ACT7/GUS* expression in the epidermis and cortex of these roots was significantly reduced, but the primordia-like structures displayed very intense GUS staining. In contrast to the above hormones, GA_3 (Fig. 7F) and hydroxyurea (data not shown) produced no significant changes in either root morphology or the expression pattern of the *ACT7/GUS* construct. All three transgenic lines responded similarly.

DISCUSSION

ACT7 Is Preferentially Expressed in Developing Tissues

Actin and other cytoskeletal proteins are often thought of as constitutively expressed "housekeeping" proteins. However, the results from this study demonstrate that *ACT7* is regulated differentially during Arabidopsis development in a very complex pattern and that *ACT7* expression is differentially influenced by a number of stimuli. The *ACT7/GUS* reporter gene was strongly expressed in a wide variety of developing tissues in which cells are rapidly dividing and elongating, but its activity was noticeably curtailed as tissue development reached completion. This link of *ACT7* expression to development was further supported by assays demonstrating that the high *ACT7/GUS*-specific activity (units/mg protein) in young leaves dropped significantly in more mature leaves. Furthermore, *ACT7/GUS* expression was protracted in tissues and cell types in which development was protracted (e.g. the hypocotyl in etiolated seedlings, vascular tissue, trichomes, and stomata).

Given the low level of *ACT7* RNA in total pollen RNA preparations and the fact that at least five other Arabidopsis actin genes are strongly expressed during late pollen development (An et al., 1996; Huang et al., 1996; S. Huang, Y.-q. An, J. McDowell, E. McKinney, R. Meagher, unpublished data), it seemed possible that *ACT7* expression in the pollen was superfluous. We were surprised, therefore, to observe *ACT7/GUS* activity late in the development of pollen in 15 of the 17 plants examined. The discrepancy between GUS and northern expression in mature pollen could result from ectopic expression of the *ACT7/GUS* fusion in pollen, as has been suggested for other promoter/GUS fusions (Uknes et al., 1993). An alternative view is that the position of the normal *ACT7* gene in the genome might "repress" pollen expression, as it did in the 2 of 17 plants showing no pollen expression. The rise in *ACT7* mRNA could be so transient that it is not measured in total pollen RNA preparations. The *ACT7/GUS* construct was made as a translational fusion that included an intact mRNA leader exon and leader intron and the first 19 codons of *ACT7*. Thus, *ACT7/GUS* expression in all tissues may also be influenced by a number of posttranscriptional factors that affect the splicing of intron L, the translational efficiency and differential stability of the fusion mRNA, and/or protein stability. With the exception of data for pollen, the mRNA steady-state data and GUS expression data are in strong agreement.

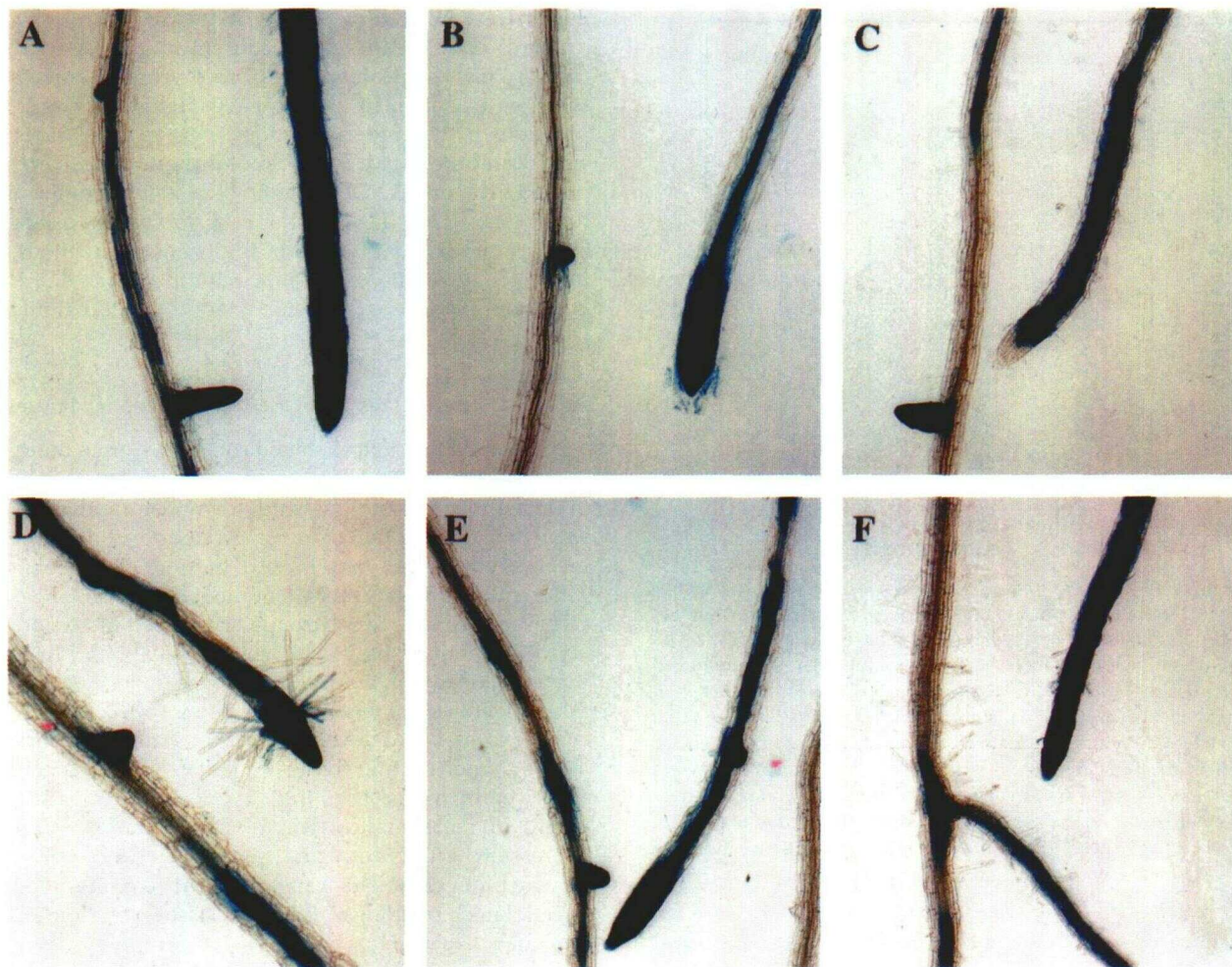


Figure 7. Histochemical localization of *ACT7/GUS* expression in the roots of transgenic *Arabidopsis* plants after treatment for 48 h with various phytohormones (see "Results"). A, Untreated control; B, IPA; C, ABA; D, 2,4-D; E, IAA; F, GA_3 .

Exogenous Hormones Alter the Pattern of *ACT7/GUS* Expression

Because phytohormones have a multitude of effects on plant development, it was expected that *ACT7* expression, which is associated with tissue growth and differentiation, would respond to hormone treatment. The experiments summarized in Figure 7 demonstrated that several exogenously applied phytohormones do indeed alter *ACT7* transcriptional regulation. Several hormones produced distinct spatial alterations in *GUS* expression consistent with the hormone's known effect on root development. ABA, considered a "stress hormone," has been shown to inhibit root growth by decreasing activity in the meristematic zone (Robertson et al., 1990). This effect is consistent with the observed inhibition of *ACT7/GUS* expression in the root meristematic zone by exogenous ABA. In addition, *ACT7/GUS* was fully active in lateral root primordia, which is consistent with Schnall and Quatrano's (1992) observation that exogenous ABA inhibits *Arabidopsis* root elongation but does not affect lateral root initiation. Both endogenous and exogenously applied cytokinins are also known to inhibit root growth (Medford et al., 1989; Su and Howell,

1992). As shown in Figure 7B, exogenous IPA dramatically inhibits *ACT7/GUS* expression in all root tissues except for the meristematic zone and the first part of the elongation zone. This observation is consistent with previous studies that suggest that cytokinins inhibit root growth via a reduction in cell elongation (Hinchee, 1981; Medford et al., 1989). Exposure to both synthetic and natural auxins inhibited *GUS* expression in the epidermis and cortex, but activated *GUS* expression in lateral root primordia-like structures that proliferated under auxin treatment. This effect was again consistent with the inhibition of root elongation and stimulation of lateral root initiation that results from auxin treatment (Estelle and Klee, 1994). In contrast, neither GA_3 nor the cell-division inhibitor hydroxyurea had a significant effect on *ACT7/GUS* expression. The latter result suggests that, unlike genes such as *cdc2A* (Hemerly et al., 1993), *ACT7* expression may not be linked to cell-cycle control.

Several features of the *ACT7/GUS* patterns of expression are seen in other hormonally regulated genes (Rodrigues-Pousada et al., 1993; Wyatt et al., 1993). The physiological relevance of exogenous hormone application experiments

is difficult to interpret because of the potential variability in uptake and transport, unknown interactions with endogenous hormones, and our lack of knowledge about the tissue-specific influences of some hormones. The effects we describe were clearly manifested after 48 h of hormone treatment; we have not yet monitored the *ACT7/GUS* response immediately after hormone addition on an hourly basis. Cytological studies have established that exogenous hormones can dramatically affect cytoskeletal architecture over much shorter times (Staiger and Lloyd, 1991; Shibaoka, 1994), and one might predict that changes in cell architecture direct the developmental changes that follow. These preliminary experiments suggest that cytoskeletal rearrangements could be linked to changes in *ACT7* gene expression. In other words, *ACT7* activity may direct the responses to these hormones.

It is interesting that each hormone provoked a distinctly different alteration in *ACT7/GUS* activity, suggesting that the *ACT7* promoter responds to several distinct developmental programs and that *ACT7* expression is subject to combinatorial control from a number of different regulators (Dickinson, 1988; Benfey et al., 1990a, 1990b; Benfey and Chua, 1990). Comparisons of *ACT7/GUS* expression in various hormone-deficient or hormone-insensitive genetic backgrounds, in combination with *ACT7* promoter dissections, should provide additional insight into the mechanisms of *ACT7* regulation.

The *ACT7* Promoter May Contain a High Density of Hormone Response Elements

A survey of the various DNA sequence databases for sequence motifs that might be contained within the 5' region of *ACT7* revealed a remarkably large number of *cis* sequences similar to phytohormonally regulated plant DNA elements. These sequences were concentrated in the promoter region immediately upstream of the TATA box and none were found within intron L. Two potential elements (GARE #1 and GARE #2, Fig. 1F) with 9 out of 12 bp of identity to the GARE found in barley α -amylase promoters (Skriver et al., 1991; Giraudat et al., 1994) were found approximately 410 and 170 bp upstream of the *ACT7* TATA box, respectively. Two more potential elements, GARE #3 and GARE #4, with 8 out of 11 bp of identity to GAREs in a wheat α -amylase promoter (Huttley and Baulcombe, 1989), were located approximately 120 and 20 bp upstream of the TATA box, respectively. An element with an 11-out-of-12-bp-match with a characterized auxin responsive element (Liu et al., 1994) was found 44 nt upstream of the TATA box. Although the two halves of the previously characterized element, 5'TGTCTC-N₃-AATAAG, are separated by only 3 bp, the two halves of the *ACT7* element are separated by 22 bp. A rotational palindrome, 5'TGTCTCTC-CCA-N₁₂-TGGGAAATAAT (underlined here and in Fig. 1F), located between and immediately flanking the two halves of the *ACT7* auxin responsive element, could anneal to bring both auxin-responsive-element components together. Two *cis* sequences, nod #1 and nod #2 (Fig. 1F), containing 7 of 8 matched bases each to the root nodule motif 5'CTTTCCCT (Fisher et al., 1988), were found at the start of and within exon

L, respectively. One might expect such a motif to be involved in the rapid proliferation of root nodule tissue, and our data suggest that *ACT7* might respond to such a program of rapid growth. There are also sequences with 10-bp (ABRE #2, Fig. 1) (Guiltinan et al., 1990), 10-bp (ABRE #3), and 8-bp (ABRE #1) matches (Marcotte et al., 1989; Shen and Ho, 1995) to the 11-bp ABRE. Two of them (ABRE #2 and ABRE #3) are found within the first 34 bp of the *ACT7* protein coding sequence in exon 1. The binding of a transacting ABA protein factor to these latter ABRE sequences could result in the negative transcriptional regulation of *ACT7* in response to ABA in meristematic cells and more mature tissues (see "Results"). Finally, two motifs (O2S #1 and #2) with 9 out of 12 bp of identity to the O2S coupling elements are located approximately 220 and 180 bp upstream from the TATA box, respectively. These elements are required for GARE and ABRE function in barley α -amylase promoters and are similar to the binding site for opaque 2, a maize transcription factor (Lanahan et al., 1992; Rogers and Rogers, 1992). For comparison, the *ACT11* Arabidopsis actin gene, which is expressed preferentially in pollen and ovules and other reproductive tissues, contains no significant matches to any of these phytohormone response elements in the 1000 bp upstream of its TATA box (S. Huang, Y.-q. An, J. McDowell, E. McKinney, R. Meagher, unpublished data).

The Sequence and Expression Pattern of *ACT7* Is Distinct from Those of Other Arabidopsis Actin Genes

An evolutionary analysis suggested that the 10 Arabidopsis actin genes fall into two ancient classes that diverged several hundred million years ago, and that these classes subsequently split again into six ancient subclasses. The *ACT7* subclass together with the *ACT2/ACT8* subclass forms a vegetative class (An et al., 1996; McDowell et al., 1996). It is interesting that the *ACT7* subclass or clade is more closely related to genes from soybean, carrot, pea, potato, rice, and pine than it is to other Arabidopsis actin genes, including *ACT2* and *ACT8*. This clade includes the soybean genes *Sac3* and *Sac7*, which are preferentially expressed in young shoots and elongating hypocotyls and respond positively to auxin (Hightower and Meagher, 1985), and also the rice genes *RAc2* and *RAc3*, which are preferentially expressed in young seedlings (McElroy et al., 1990). Thus, *ACT7* may represent an ancient subclass of genes that diverged prior to angiosperm radiation and possibly even earlier. We propose that this ancient and hormonally regulated subclass of actin genes will be found in all higher plants and that based both on sequence divergence and patterns of gene expression, *ACT7* is the sole representative of this subclass in Arabidopsis (see below). It is tempting to speculate that the evolutionary conservation of this actin subclass reflects selection for unique actin functions or regulation in rapidly developing, hormonally responsive tissues.

In parallel with this study, we have surveyed the expression of the other expressed Arabidopsis actin genes and have found that each of the evolutionary subclasses has characteristic regulatory patterns that differ, often dramatically, from the complex pattern shown by *ACT7*. For ex-

ample, the *ACT4/12* subclass is expressed almost exclusively in postmeiotic pollen and differentiating vascular tissue (Huang et al., 1996), whereas the *ACT1/3* subclass is expressed preferentially in mature pollen and all organ primordia (An et al., 1996). The *ACT11* subclass is expressed in vascular tissue, all floral organs, and particularly in pollen, ovules, and developing embryos (S. Huang, Y.-Q. An, J. McDowell, E.C. McKinney, R.B. Meagher, unpublished data). *ACT11* is expressed most strongly in reproductive organs and tissues in which *ACT7* is not expressed and thus may complement *ACT7* expression in the whole plant. The *ACT2/8* subclass is evolutionarily the closest to *ACT7* and most similar to *ACT7* in its expression in vegetative tissues (An et al., 1996). However, *ACT2* and *ACT8* have more temporally uniform, constitutive patterns of expression than does *ACT7*. The *ACT2/GUS* and *ACT8/GUS* constructs are almost as strongly expressed in mature as in immature tissues. *ACT2* and *ACT8* mRNAs are also much more abundant in most mature vegetative tissues than is the *ACT7* message. *ACT2* and *ACT8* may provide actin for "housekeeping" functions such as cytoplasmic streaming or intercellular organization, which are required even of mature cells, whereas *ACT7* may have an exclusively developmental role.

The absence of GUS expression in developing ovules and embryos was also notable. The subsequent activation of *ACT7/GUS* in mature, dry seeds suggests that the gene may be under the control of a very late embryogenic or postdesiccation regulatory program (Roberts et al., 1993). *ACT7/GUS* activity continued to be strong in germinating seedlings. Although *ACT2/GUS* expression was strong in germinated seedlings, none of the eight other actin 5' translational GUS fusion genes we examined was strongly active in the hypocotyl and aleurone except *ACT7/GUS*. This suggests that *ACT7* is the sole source of actin for all actin-based cytoskeletal processes in these tissues and that the *ACT7* protein is not highly specialized in terms of function. *ACT7* expression may be absolutely required for germination and/or hypocotyl development.

These results on *ACT7* expression strongly support the hypothesis that plants have ancient actin subclasses that are differentially regulated. Next, we would like to determine the functional relevance of the dissimilar regulatory patterns we have observed for the various actins. The expression of at least one actin subclass, such as *ACT7*, in rapidly developing tissues is consistent with results of cytological studies that show that the cytoskeleton is very dynamic during cellular morphogenesis, forming a number of structurally distinct and functionally specialized arrays in dividing (Mineyuki and Palevitz, 1990; Eleftheriou and Palevitz, 1992), elongating (Thimann et al., 1992; Thimann and Biradivolu, 1994), and differentiating cells (Jung and Wernicke, 1991; Seagull and Falconer, 1991). It seems unlikely that the *ACT7* protein isoform is functionally specialized, so the *ACT7* gene could simply provide increased quantities of actin for these diverse tasks in cells undergoing rapid growth and development. We hope to test the functional significance of *ACT7* expression in the future

with the characterization of the *ACT7* protein and an examination of the phenotypes associated with *ACT7* mutations (McKinney et al., 1995).

ACKNOWLEDGMENTS

We gratefully acknowledge the comments of Katherine Spindler, Marcus Fechheimer, Dmitry Belostotsky, Angela Vitale, Susan Wessler, and Gay Gragson on the manuscript. Ralph Quatrano and Joaquin Medina were helpful in identifying phytohormonally regulated *cis*-DNA motifs.

Received November 29, 1995; accepted April 19, 1996.

Copyright Clearance Center: 0032-0889/96/111/0699/13.

The GenBank accession number for the *ACT7* genomic sequence is U27811.

LITERATURE CITED

- An G, Ebert PR, Mitra A, Ha SB (1988) Binary vectors. In SB Gelvin, RA Schilperoot, eds, *Plant Molecular Biology*. Martinus Nijhoff, Amsterdam, pp 1-19
- An Y-Q, Huang S, McDowell JM, McKinney EC, Meagher RB (1996) The Arabidopsis *ACT1/ACT3* actin subclass is expressed in organ primordia and mature pollen. *Plant Cell* 8: 15-30
- Baird WV, Meagher RB (1987) A complex gene superfamily encodes actin in petunia. *EMBO J* 6: 3223-3231
- Benfey P, Ren L, Chua N-H (1990a) Combinatorial and synergistic properties of CaMV 35S enhancer domains. *EMBO J* 9: 1685-1696
- Benfey PN, Chua N-H (1990) The CaMV 35S promoter and combinatorial regulation of transcription in plants. *Science* 250: 959-966
- Benfey PN, Ren L, Chua N-H (1990b) Tissue-specific expression from CaMV 35S enhancer subdomains in early stages of plant development. *EMBO J* 9: 1677-1684
- Bradford MM (1976) A rapid and sensitive method for the quantitation of microgram quantities of protein utilizing the principle of protein-dye binding. *Anal Biochem* 72: 248-254
- Brown RC, Lemmon BE (1985) Development of stomata in *Selaginella*: division polarity and plastid movements. *Am J Bot* 72: 1914-1925
- Cho S-O, Wick SM (1991) Actin in the developing stomatal complex of winter rye: a comparison of actin antibodies in Rh-phalloidin labeling of control and CB-treated tissues. *Cell Motil* 19: 25-36
- Dickinson WJ (1988) On the architecture of regulatory systems: evolutionary insights and implications. *BioEssays* 8: 204-208
- Dolan L, Janmaat K, Willemsen V, Linstead P, Poethig S, Roberts K, Scheres B (1993) Cellular organization of the *Arabidopsis thaliana* root. *Development* 119: 71-84
- Drouin G, Dover GA (1990) Independent gene evolution in the potato actin gene family demonstrated by phylogenetic procedures for resolving gene conversions and the phylogeny of angiosperm actin genes. *J Mol Evol* 31: 132-150
- Eleftheriou EP, Palevitz BA (1992) The effect of cytochalasin D on preprophase band organization in root tip cells of *Allium*. *J Cell Sci* 103: 989-998
- Estelle M, Klee HJ (1994) Auxin and cytokinin in Arabidopsis. In EM Meyerowitz, CR Somerville, eds, *Arabidopsis*. Cold Spring Harbor Laboratory Press, Cold Spring Harbor, NY, pp 555-578
- Feinberg AP, Vogelstein B (1983) A technique for radiolabelling DNA restriction endonuclease fragments to high specific activity. *Anal Biochem* 132: 6-13, addendum
- Fisher RF, Egelhoff TT, Mulligan JT, Long SR (1988) Specific binding of proteins from *Rhizobium meliloti* cell-free extracts containing NodD to DNA sequences upstream of inducible nodulation genes. *Genes Dev* 2: 282-293
- Giraudat J, Parcy F, Bertauche N, Gosti F, Leung J, Morris P, Bouvier-Durand M, Vartanian N (1994) Current advances in abscisic acid action and signalling. *Plant Mol Biol* 26: 1557-1577

- Guiltinan MJ, Marcotte WR, Quatrano RS (1990) A plant leucine zipper protein that recognizes an abscisic acid response element. *Science* **250**: 267–271
- Hemerly AS, Ferreira P, Engler JD, Van Montagu M, Engler G, Inze D (1993) *cdc2a* expression in Arabidopsis is linked with competence for cell division. *Plant Cell* **5**: 1711–1723
- Hightower RC, Meagher RB (1985) Divergence and differential expression of soybean actin genes. *EMBO J* **4**: 1–8
- Hightower RC, Meagher RB (1986) The molecular evolution of actin. *Genetics* **114**: 315–332
- Hinchee MAW (1981) Morphogenesis of aerial and subterranean roots of *Monstra deliciosa*. *Bot Gaz* **142**: 347–359
- Huang S, An Y-Q, McDowell J, McKinney EC, Meagher RB (1996) The Arabidopsis ACT4/ACT12 actin gene subclass is strongly expressed in post-mitotic pollen. *Plant J* (in press)
- Huttley A, Baulcombe D (1989) A wheat α -Amy2 promoter is regulated by gibberellin in transformed oat aleurone protoplasts. *EMBO J* **8**: 1907–1913
- Jefferson RA, Kavanagh TA, Bevan MW (1987) GUS fusions: β -glucuronidase as a sensitive and versatile gene fusion marker in higher plants. *EMBO J* **6**: 3901–3907
- Jung G, Wernicke W (1991) Patterns of actin filaments during cell shaping in developing mesophylls of wheat (*Triticum aestivum* L.). *Eur J Cell Biol* **56**: 139–146
- Lanahan M-H, Rogers S, Rogers J (1992) A gibberellin response complex in cereal α amylase gene promoters. *Plant Cell* **4**: 203–211
- Liu Z-B, Ulmasov T, Shi X, Hagen G, Guilfoyle TJ (1994) Soybean GH3 promoter contains multiple auxin-inducible elements. *Plant Cell* **6**: 645–657
- Lloyd C (1991) Probing the plant cytoskeleton. *Nature* **350**: 189–190
- Logemann J, Schell J, Willmitzer L (1987) Improved method of isolation of RNA from plant tissues. *Anal Biochem* **163**: 16–20
- Marcotte W, Russell S, Quatrano R (1989) Abscisic acid responsive sequences from the Em gene of wheat. *Plant Cell* **1**: 969–976
- Marton L, Browse J (1991) Facile transformation of Arabidopsis. *Plant Cell Rep* **10**: 235–239
- McDowell JM, Huang S, McKinney EC, An Y-Q, Meagher RB (1996) Arabidopsis thaliana contains ten actin genes encoding six ancient protein subclasses. *Genetics* **142**: 587–602
- McElroy D, Rothenberg M, Reece KS, Wu R (1990) Characterization of the rice (*Oryza sativa*) actin gene family. *Plant Mol Biol* **15**: 257–268
- McKinney EC, Ali N, Traut A, Feldmann KA, Belostotsky DA, McDowell JA, Meagher RB (1995) Sequence based identification of T-DNA insertion mutations in Arabidopsis: actin mutants *act2-1* and *act4-1*. *Plant J* **8**: 613–622
- Meagher RB (1991) Divergence and differential expression of actin gene families in higher plants. *Int Rev Cytol* **125**: 139–163
- Meagher RB, McLean BG (1990) Diversity of plant actins. *Cell Motil* **16**: 164–166
- Meagher RB, Williamson RE (1994) The plant cytoskeleton. In E Meyerowitz, C Somerville, eds, *Arabidopsis*. Cold Spring Harbor Laboratory Press, Cold Spring Harbor, NY, pp 1049–1084
- Medford JI, Horgan R, El-Sawi Z, Klee HJ (1989) Alterations of endogenous cytokinins in transgenic plants using a chimeric isopentyl transferase gene. *Plant Cell* **1**: 403–413
- Mineyuki Y, Palevitz BA (1990) Relationship between preprophase band organization, F-actin and the division site in *Allium*. Fluorescence and morphometric studies on cytochalasin-treated cells. *J Cell Sci* **97**: 283–295
- Nagao RT, Shah DM, Eckenrode VK, Meagher RB (1981) Multi-gene family of actin-related sequences isolated from soybean genomic library. *DNA* **2**: 1–9
- Nairn CJ, Winesett L, Ferl RJ (1988) Nucleotide sequence of an actin gene from Arabidopsis thaliana. *Gene* **65**: 247–257
- Parthasarathy MV, Perdue TD, Witzmun A, Alvernaz J (1985) Actin network as a normal component of the cytoskeleton in many vascular plant cells. *Am J Bot* **72**: 1318–1323
- Pearson L, Meagher RB (1990) Diverse soybean actin transcripts contain a large intron in the 5' untranslated leader: structural similarity to vertebrate muscle actin genes. *Plant Mol Biol* **14**: 513–526
- Roberts JK, DeSimone NA, Lingle WL, Dure LI (1993) Cellular concentrations and uniformity of cell-type accumulation of two lea proteins in cotton embryos. *Plant Cell* **5**: 769–780
- Robertson JM, Hubick KT, Yeung EC, Reid DM (1990) Developmental responses to drought and abscisic acid in sunflower roots. *J Exp Bot* **41**: 325–337
- Rodrigues-Pousada RA, De Rycke R, Dedonder A, Van Caeneghem W, Engler G, Van Montagu M, Van Der Straeten D (1993) The Arabidopsis 1-aminocyclopropane-1-carboxylate synthase gene is expressed during early development. *Plant Cell* **5**: 897–911
- Rogers JC, Rogers SW (1992) Definition and functional implications of gibberellin and abscisic acid cis-acting hormone response complexes. *Plant Cell* **4**: 1443–1451
- Sambrook J, Fritsch EF, Maniatis T (1989) *Molecular Cloning: A Laboratory Manual*. Cold Spring Harbor Laboratory Press, Cold Spring Harbor, NY, p 900
- Schiefelbein J, Benfey P (1991) The development of plant roots: new approaches to underground problems. *Plant Cell* **3**: 1147–1154
- Schnall JS, Quatrano RS (1992) Abscisic acid elicits the water-stress response in root hairs of Arabidopsis thaliana. *Plant Physiol* **100**: 216–218
- Seagull R, Falconer M, Weerdenburg C (1987) Microfilaments: dynamic arrays in higher plant cells. *J Cell Biol* **104**: 995–1004
- Seagull RW (1989) The plant cytoskeleton. *CRC Crit Rev Plant Sci* **8**: 131–167
- Seagull RW, Falconer MM (1991) In vitro xylogenesis. In CW Lloyd, ed, *The Cytoskeletal Basis of Plant Growth and Form*. Academic Press, London, pp 183–194
- Shen Q, Ho T-H (1995) Functional dissection of an ABA-inducible gene reveals two independent ABA-responsive complexes each containing a G-box and a novel cis acting element. *Plant Cell* **7**: 295–307
- Shibaoka H (1994) Plant hormone-induced changes in the orientation of cortical microtubules. *Annu Rev Plant Physiol Plant Mol Biol* **45**: 527–544
- Skriver K, Olsen F, Rogers J, Mundy J (1991) Cis-acting DNA elements responsive to gibberellin and its antagonist abscisic acid. *Proc Natl Acad Sci USA* **88**: 7266–7270
- Smyth DR, Bowman JL, Meyerowitz EM (1990) Early flower development in Arabidopsis. *Plant Cell* **2**: 755–767
- Staiger CJ, Lloyd CW (1991) The plant cytoskeleton. *Curr Opin Cell Biol* **3**: 33–42
- Staiger CJ, Schliwa M (1987) Actin localization and function in higher plants. *Protoplasma* **141**: 1–12
- Su W, Howell SH (1992) A single genetic locus, *Ckr1*, defines Arabidopsis mutants in which root growth is resistant to low concentrations. *Plant Physiol* **99**: 1569–1574
- Tanzer MM, Meagher RB (1994) Faithful degradation of soybean *rbcs* mRNA in vitro. *Mol Cell Biol* **14**: 2640–2650
- Thangavelu M, Belostotsky D, Bevan MW, Flavell RB, Rogers HJ, Lonsdale DM (1993) Partial characterization of the Nicotiana tabacum actin gene family: evidence for pollen specific expression of one of the gene family members. *Mol Gen Genet* **240**: 290–295
- Thimann K, Biradivolu R (1994) Actin and the elongation of plant cells. 2. The role of divalent ions. *Protoplasma* **183**: 5–9
- Thimann KV, Reese K, Nachmais VT (1992) Actin and the elongation of plant cells. *Protoplasma* **171**: 153–166
- Thompson DM, Tanzer MM, Meagher RB (1992) Degradation products of the mRNA encoding the small subunit of ribulose-1,5-bisphosphate carboxylase in soybean and transgenic petunia. *Plant Cell* **4**: 47–58
- Uknes S, Dincher S, Friedrich L, Negrotto D, Williams S, Thompson-Taylor H, Potter S, Ward E, Ryals J (1993) Regulation of pathogenesis-related protein-1a gene expression in tobacco. *Plant Cell* **5**: 159–169
- Wyatt RE, Ainley WM, Nagao RT, Conner TW, Key JL (1993) Expression of the Arabidopsis AtAux 2-11 auxin-responsive gene in transgenic plants. *Plant Mol Biol* **22**: 731–749
- Zhang W, McElroy D, Wu R (1991) Analysis of rice *Act1* 5' region activity in transgenic rice plants. *Plant Cell* **3**: 1155–1165